Published in final edited form as:
Cell. 2009 March 6; 136(5): 939–951. doi:10.1016/j.cell.2009.01.025.

A PP2A regulatory subunit PPTR-1 regulates the *C. elegans* Insulin/IGF-1 signaling pathway by modulating AKT-1 phosphorylation

Srivatsan Padmanabhan[1,2], **Arnab Mukhopadhyay**[1,2,3], **Sri Devi Narasimhan**[1,2], **Gregory Tesz**[4], **Michael P. Czech**[4], and **Heidi A. Tissenbaum**[*,2,4]

[2] Program in Gene Function and Expression, University of Massachusetts Medical School, 364 Plantation Street, Worcester, MA 01605

[4] Program in Molecular Medicine, University of Massachusetts Medical School, 364 Plantation Street, Worcester, MA 01605

Summary

The *C. elegans* insulin/IGF-1 signaling (IIS) cascade plays a central role in the regulation of lifespan, dauer diapause, metabolism and stress response. The major regulatory control of IIS is through phosphorylation of its components by serine/threonine-specific protein kinases. In a RNAi screen for serine/threonine protein phosphatases that counter-balance the effect of the kinases in the IIS pathway, we identified *pptr-1*, a B56 regulatory subunit of the PP2A holoenzyme. Modulation of *pptr-1* affects phenotypes associated with the IIS pathway including lifespan, dauer, stress resistance and fat storage. We show that PPTR-1 functions by regulating worm AKT-1 phosphorylation at Thr 350. With striking conservation, mammalian B56β regulates Akt phosphorylation at Thr 308 in 3T3-L1 adipocytes. In *C. elegans*, this modulation ultimately leads to changes in subcellular localization and transcriptional activity of the forkhead transcription factor DAF-16. This study reveals a conserved role for the B56 regulatory subunit in modulating insulin signaling through AKT dephosphorylation and thereby has widespread implications in cancer and diabetes research.

Introduction

The insulin/IGF-1-like signaling (IIS) pathway is an evolutionarily conserved neuro-endocrine pathway that regulates metabolism, development, stress resistance and lifespan (Antebi, 2007; Barbieri et al., 2003; Kenyon, 2005; Wolff and Dillin, 2006). In *Caenorhabditis elegans* (*C. elegans*), the insulin-like receptor DAF-2 (Kimura et al., 1997) signals through a PI 3-kinase (AGE-1/AAP-1) (Morris et al., 1996; Wolkow et al., 2002) signaling cascade that activates the downstream serine/threonine kinases PDK-1, AKT-1, AKT-2 and SGK-1 (Hertweck et al., 2004; Paradis et al., 1999; Paradis and Ruvkun, 1998). These kinases in turn function to negatively regulate the forkhead transcription factor (FOXO), DAF-16 (Lin et al., 1997; Ogg et al., 1997).

*Corresponding author, e.mail: E-mail: heidi.tissenbaum@umassmed.edu.
[1]These authors contributed equally
[3]Current Address: National Institute of Immunology, Aruna Asaf Ali Marg, New Delhi 110067 India

Reduction-of-function mutations in serine/threonine kinases upstream of DAF-16 lead to changes in lifespan, development, metabolism and/or stress resistance (Antebi, 2007; Kenyon, 2005; Wolff and Dillin, 2006). Importantly, loss-of-function mutations in *daf-16* completely suppress these phenotypes (Antebi, 2007; Kenyon, 2005; Mukhopadhyay et al., 2006; Wolff and Dillin, 2006). Thus DAF-16 is a major downstream target of the IIS pathway. Regulation of DAF-16 by AKT-1, AKT-2 and SGK-1 results in its nuclear exclusion and sequestration in the cytosol (Lin et al., 2001) (Hertweck et al., 2004; Lee et al., 2001). In contrast, under low signaling conditions, active DAF-16 enters the nucleus and transactivates or represses its direct target genes (Henderson and Johnson, 2001; Hertweck et al., 2004; Lee et al., 2001; Lin et al., 2001; Oh et al., 2006). Strikingly, this negative regulation of FOXO/DAF-16 is conserved across species. In mammals, the Akt and SGK kinases can phosphorylate and negatively regulate FOXO (Brunet et al., 1999; Brunet et al., 2001).

Although regulation of the IIS pathway by serine/threonine protein kinases has been extensively studied, little is known about the phosphatases acting in this pathway. In *C. elegans*, the lipid phosphatase DAF-18 (homologous to mammalian Phosphatase and Tensin Homolog, PTEN) is the only phosphatase that has been identified and characterized as a negative regulator of the IIS pathway (Gil et al., 1999; Mihaylova et al., 1999; Ogg and Ruvkun, 1998; Rouault et al., 1999). The increased lifespan of *daf-2* mutant worms is suppressed by loss-of-function mutation in *daf-18* (Dorman et al., 1995; Larsen et al., 1995). Therefore, to identify additional regulators of the IIS pathway, we performed a directed RNAi screen of serine/threonine protein phosphatases that affect phenotypes regulated by the IIS pathway.

C. elegans development proceeds from an egg, through 4 larval stages into a self-fertilizing, hermaphrodite adult. However, under unfavorable growth conditions such as crowding and low food availability, worms enter a stage of diapause known as dauer (Riddle D., 1997). Upon favorable growth conditions, dauers are able to form reproductive adults. Since worms form dauers constitutively when the function of IIS pathway is reduced by mutations, we took advantage of a temperature-sensitive (ts) allele of *daf-2* for the RNAi screen (Riddle et al., 1981). We screened for genes that suppressed dauer formation in *daf-2(e1370)* mutants. In this report, we characterize PPTR-1, a regulatory subunit of the PP2A holoenzyme, as an important regulator of development, longevity, metabolism and stress response in *C. elegans*. We show that PPTR-1 acts by modulating AKT-1 phosphorylation and as a consequence controls DAF-16 activity.

Results

RNAi screen to identify phosphatases in IIS pathway

To identify the serine/threonine phosphatases in the *C. elegans* genome, we performed *in silico* analyses using both NCBI KOGs (clusters of euKaryotic Orthologous Groups) and WormBase (a *C. elegans* database: http://www.wormbase.org; WS152) annotations. A total of 60 genes were identified for further analysis (Figure 1A). We obtained RNAi clones for these phosphatases from the Ahringer RNAi library (Kamath et al., 2003), generated them using available clones from the ORFeome library (Reboul et al., 2003) or cloned them *de-novo* using Gateway Technology (Invitrogen, USA; Materials and Methods). We were unable to clone 3 of the phosphatase cDNAs and therefore screened a total of 57 candidates.

In addition, we included 6 of the 7 annotated PP2A holoenzyme regulatory subunits (one was not cloned) in the screen for two reasons. First, a preliminary chemical inhibitor screen identified the PP2A family of phosphatases as important regulators of DAF-16 nuclear translocation (Padmanabhan and Tissenbaum, unpublished data). Second, the PP2A holoenzyme is comprised of a catalytic, structural and a regulatory subunit (Janssens et al.,

2008) and RNAi of the catalytic and structural subunits of PP2A resulted in lethality (data not shown).

daf-2(e1370) carries a mutation in the insulin receptor tyrosine kinase domain that results in a ts phenotype for dauer formation (Kimura et al., 1997). *daf-2(e1370)* worms arrest as 100% dauers at 25°C whereas at 15°C they have a normal reproductive cycle (Riddle D., 1997). At an intermediate temperature of 20 °C, a significant percentage of *daf-2(e1370)* worms form dauers. Therefore, at this temperature, one can use RNAi to easily assess the contribution of any gene in modulating *daf-2* dauer formation.

For the screen, *daf-2(e1370)* mutants were grown on RNAi-expressing bacteria for two generations, and eggs were picked onto 3 plates for each RNAi clone (Figure 1B). The plates were incubated at 20°C and scored 3.5-4 days later for the presence of dauers and non-dauers. Since DAF-18 is the only known phosphatase that negatively regulates the IIS in *C. elegans*, we used *daf-18* RNAi as a positive control in all our experiments. From a total of 63 RNAi clones (57 phosphatases and 6 regulatory subunits), we identified two phosphatases that dramatically decreased *daf-2(e1370)* dauer formation to a level similar to *daf-18* RNAi (Figure 1C).

Our top candidate, *fem-2* (T19C3.4) functions in *C. elegans* sex determination (Kimble et al., 1984; Pilgrim et al., 1995). However, further analysis with an additional *daf-2* allele, *daf-2 (e1368)*, revealed that *fem-2* RNAi suppresses dauer formation in an allele-specific manner. *fem-2* RNAi suppressed dauer formation of *daf-2(e1370)* but not *daf-2(e1368)* (data not shown) and therefore, we focused on the next top candidate.

pptr-1 (W08G11.4), the next candidate, is a member of the B56 family of genes encoding regulatory subunits of the PP2A protein phosphatase holoenzyme. The *C. elegans* genome contains 7 known PP2A regulatory subunit genes (*pptr-1* and *pptr-2*, B56 family; *sur-6*, B55 family; F47B8.3, C06G1.5, *rsa-1* and T22D1.5, B72 family; currently F47B8.3 is not annotated as a PP2A regulatory subunit according to WormBase Release WS194). To determine the specificity of *pptr-1* in regulating dauer formation, we re-tested the six PP2A regulatory subunits included in the screen for their ability to regulate dauer formation in *daf-2(e1370)* mutants. Knockdown efficiency of each RNAi clone was verified by RT PCR (Supplemental Table 1A). As shown in Figure 1D and Supplemental Table 1A and 1B, only *pptr-1* RNAi suppressed *daf-2(e1370)* dauer formation comparable to *daf-18* RNAi.

We next analyzed the effect of *pptr-1* RNAi on dauer formation of *daf-2(e1368)*. *pptr-1* RNAi significantly suppressed the dauer formation of *daf-2(e1368)* (69.2 ± 9.4 % on vector RNAi versus 3.8 ± 4.4% on *pptr-1* RNAi; Table 1 and Supplemental Table 2). Therefore the effect of *pptr-1* RNAi on *daf-2* mutants is not allele-specific. Together these results indicate that *pptr-1* may function downstream of *daf-2*. In addition, *pptr-1* is the only PP2A regulatory subunit to affect *daf-2* dauer formation.

pptr-1 regulates dauer formation through the IIS pathway

To further investigate the role of *pptr-1* in dauer formation, we performed genetic epistasis analysis. In addition to the *C. elegans* IIS pathway, a second parallel TGF-β pathway also regulates dauer formation (Patterson and Padgett, 2000; Savage-Dunn, 2005). In this pathway, loss of function mutations in *daf-7* (TGF- β ligand), *daf-1* and *daf-4* (receptors) or *daf-14* and *daf-8* (R-Smads) lead to constitutive dauer formation; loss-of-function mutations in *daf-3* (Co-Smad) or *daf-5* (Sno/Ski) suppress these phenotypes (da Graca et al., 2004; Gunther et al., 2000; Inoue and Thomas, 2000; Patterson et al., 1997; Ren et al., 1996). However, mutations in *daf-3* do not suppress *daf-2(e1370)* dauer formation (Vowels and Thomas, 1992). We generated a *daf-2(e1370);daf-3(mgDf90)* double mutant, which bears a null mutation in

daf-3 (Patterson et al., 1997) which essentially removes the input from the TGF- β pathway for dauer formation. In this strain, the dauer formation of *daf-2(e1370);daf-3(mgDf90)* worms was suppressed by *pptr-1* RNAi (94.5 ± 0.8 % dauers on vector RNAi to 42.7 ± 14.6. % dauers on *pptr-1* RNAi; Table 1 and Supplemental Table 2). This data suggests that *pptr-1* controls dauer formation specifically through the IIS pathway and not the TGF-β pathway.

pptr-1 affects longevity, metabolism and stress response downstream of the IIS receptor

In addition to dauer formation, the *C. elegans* IIS pathway also regulates lifespan, fat storage and stress resistance (Antebi, 2007; Kenyon, 2005; Wolff and Dillin, 2006). Since *pptr-1* regulates dauer formation specifically via the IIS pathway, we next determined whether this gene could also affect these other important phenotypes.

Mutations in *daf-2* result in lifespan extension (Kenyon et al., 1993) that is suppressed by loss-of-function mutations in *daf-18* (Dorman et al., 1995; Larsen et al., 1995). To investigate whether *pptr-1* can regulate lifespan similar to *daf-18*, we determined whether knocking down *pptr-1* by RNAi could affect *daf-2(e1370)* lifespan. We grew wild type and *daf-2(e1370)* worms on vector, *daf-18* and *pptr-1* RNAi and measured lifespan (Figure 2A). Similar to *daf-18* RNAi, knockdown of *pptr-1* resulted in a significant reduction in *daf-2(e1370)* lifespan (mean lifespan of *daf-2(e1370)* on vector RNAi is 33.9 ± 0.7 days, on *pptr-1* RNAi is 27.7 ± 0.9 days and on *daf-18* RNAi is 20.4 ± 0.6 days, p value < 0.0001; Figure 2A and Supplemental Table 3A). In contrast, lifespan of wild type was unaffected by *pptr-1* RNAi (mean lifespan of wild type on vector RNAi is 22.8 ± 0.4 days, is 21.9 ± 0.5 days on *pptr-1* RNAi and 18.6 ± 0.3 days on *daf-18* RNAi; Figure 2B and Supplemental Table 3A). Thus, *pptr-1* affects lifespan in addition to dauer formation.

Lifespan extension correlates well with increased stress resistance (Lithgow and Walker, 2002; Oh et al., 2005). For example, *daf-2(e1370)* mutants are not only long-lived but are also extremely resistant to various stresses such as heat and oxidative stress (Honda and Honda, 1999; Lithgow et al., 1995; Munoz and Riddle, 2003). Therefore, we next analyzed the effect of *pptr-1* RNAi on the thermotolerance of *daf-2(e1370)* mutants. As anticipated, *pptr-1* RNAi significantly reduced the thermotolerance of *daf-2(e1370)* mutants (on vector RNAi, *daf-2 (e1370)* had a mean survival of 15.2 ± 0.7 hrs, whereas on *pptr-1* RNAi survival was 13.8 ± 0.5 hrs (p value< 0.006). *pptr-1* RNAi did not affect the thermotolerance of wild type worms; mean thermotolerance was 9.8 ± 0.4 hrs on vector RNAi, versus 9.3 ± 0.3 hrs on *pptr-1* RNAi; Figure 2C and Supplemental Table 4).

In addition to enhanced lifespan and stress resistance, *daf-2* mutants have increased fat storage (Ashrafi et al., 2003; Kimura et al., 1997). We next asked whether *pptr-1* could also affect fat storage in wild type and *daf-2(e1370)* worms using Sudan black staining. Consistent with our lifespan and stress resistance results, *pptr-1* RNAi suppressed the increased fat storage of *daf-2 (e1370)* without affecting wild type fat storage (Figure 2D). Finally, *daf-2* mutants have a slow growth phenotype (Gems et al., 1998; Jensen et al., 2007) that is suppressed by knockdown of *daf-16* by RNAi (Supplemental Table 5). Similar to *daf-16* RNAi and *daf-18* RNAi, *pptr-1* RNAi suppresses this slow growth phenotype. Together, these experiments suggest that *pptr-1* regulates multiple phenotypes associated with the IIS pathway in *C. elegans*.

pptr-1 functions at the level of *akt-1*

Signals from DAF-2 are transduced to the PI 3-kinase AGE-1 to activate the downstream serine/threonine kinase PDK-1. PDK-1 activates three downstream serine/threonine kinases, AKT-1, AKT-2 and SGK-1 (Antebi, 2007; Kenyon, 2005; Wolff and Dillin, 2006). These kinases together regulate the transcription factor DAF-16 by direct phosphorylation (Hertweck et al., 2004). Mutations in *daf-16* suppress the enhanced dauer formation of *pdk-1* (Paradis et

al., 1999) or *akt-1*/*akt-2* mutants (Oh et al., 2005; Paradis and Ruvkun, 1998). Thus far, our analysis suggests that *pptr-1* functions in the IIS pathway. We sought to identify the potential target of *pptr-1* by performing genetic epistasis experiments on components of the IIS pathway.

First we analyzed the effect of *pptr-1* RNAi on dauer formation of a *pdk-1* mutant. Dauer formation of *pdk-1(sa680)* was suppressed by *pptr-1* RNAi (95.6 ± 1.0 % dauers on vector RNAi versus 9.5 ± 0.3 % dauers on *pptr-1* RNAi, Table 1 and Supplemental Table 2). In contrast, *daf-18* RNAi had no effect on *pdk-1(sa680)* dauer formation (Table 1 and Supplemental Table 2). Therefore, these results place *pptr-1* downstream of *pdk-1* and are consistent with the current understanding that *daf-18* acts upstream of *pdk-1*.

Next, to investigate whether *pptr-1* acts at the level of *akt-1*, *akt-2* or *sgk-1*, we first analyzed dauer formation in *akt-1(ok525)*, *akt-2(ok393)* and *sgk-1(ok538)* single mutants and the *akt-1 (ok525);akt-2(ok393)* double mutant. While *akt-1(ok525)*, *akt-2(ok393)* and *sgk-1(ok538)* single mutants do not arrest as dauers at either 20 or 25 °C, the *akt-1(ok525);akt-2(ok393)* double mutant forms 100% dauers at all temperatures (Oh et al., 2005). To circumvent this problem, we generated double mutants of *daf-2(e1370);akt-1(ok525)*, *daf-2(e1370);akt-2 (ok393)* and *daf-2(e1370);sgk-1(ok538)* and tested these strains for dauer formation on vector, *daf-18* and *pptr-1* RNAi. We reasoned that in a *daf-2* mutant background, the *akt-1*, *akt-2* and *sgk-1* mutants would exhibit temperature-induced dauer formation. Indeed, all three double mutants were able to form dauers at 20 °C (Table 1 and Supplemental Table 2- see panel for vector RNAi). Importantly, *pptr-1* RNAi significantly suppressed dauer formation in *daf-2 (e1370);akt-2(ok393)* (36.8 ± 3.8 % dauers on vector RNAi versus 10.8 ± 4.3 % on *pptr-1* RNAi; Table 1 and Supplemental Table 2). In addition, *pptr-1* RNAi suppressed dauer formation of *daf-2(e1370);sgk-1(ok538)* worms (65.4 ± 4.9 % dauers on vector RNAi versus 0 % on *pptr-1* RNAi, Table 1 and Supplemental Table 2). In contrast, *pptr-1* RNAi did not affect dauer formation of *daf-2(e1370);akt-1(ok525)* mutants (vector RNAi is 94.8. ± 3.1 % versus 96.0 ± 1.7 % on *pptr-1* RNAi; Table 1 and Supplemental Table 2). However, *daf-18* RNAi can suppress *daf-2(e1370) akt-1(ok525)* dauer formation (reduced to 10.5 ± 0.8%; Table 1). These observations genetically place *pptr-1* at the level or downstream of *akt-1* in the IIS pathway.

PPTR-1 and AKT-1 are expressed in the same tissues

Since *pptr-1* and *akt-1* genetically interact, we wanted to investigate whether they have a common expression pattern. We generated or obtained *akt-1*::*gfp*, *akt-2*::*gfp*, *sgk-1*::*gfp* and we tagged *pptr-1* with *mCherry* and a minimal *flag* tag to generate *pptr-1*:: *mCherry-flag* transgenic worms (hence referred to as *pptr-1*::*mC-flag*; Materials and Methods; GFP/mC-FLAG refers to protein while *gfp/mC-flag* stands for transgene). We made double transgenic worms by crossing *pptr-1*::*mC-flag* worms to each of the above-mentioned GFP lines. Similar to published data, we observed AKT-1::GFP predominantly in the pharynx, several head neurons, the nerve ring, spermathecae and vulva (Paradis and Ruvkun, 1998); AKT-2::GFP in the pharynx (predominantly in the anterior region), somatic muscles, vulva muscles, spermathecae (Paradis and Ruvkun, 1998); SGK-1::GFP in amphid neurons, intestine and some tail neurons (Hertweck et al., 2004) (Figure 3A, B, C middle panel and Supplemental Figure 1). PPTR-1::mC-FLAG was also observed in the pharynx, head neurons, nerve ring, spermathecae and vulva (Figure 3A, B, C left panel and Supplemental Figure 1). To observe the sub-cellular localization of PPTR-1, we stained *pptr-1*::*mC-flag* worms with DAPI (Materials and Methods). We find that PPTR-1 is predominantly cytosolic with little DAPI overlap (Supplemental Figure 2 and Supplemental Movies). As shown in Figure 3A-C (Merge) as well as in the confocal movies (Supplemental Movies), there is remarkable overlap between the expression patterns of PPTR-1 and AKT-1. We also observed partial overlap between AKT-2::GFP and PPTR-1::mC-FLAG, predominantly in the pharynx (Figure 3B, Merge;

Supplemental Movies). SGK-1 and PPTR-1 are expressed in different tissues and we do not see any significant overlap (Figure 3C, Merge; Supplemental Movies).

PPTR-1 regulates AKT-1 phosphorylation

Given the genetic epistasis as well as the overlapping expression patterns, we next determined whether PPTR-1 directly interacts with AKT-1 by co-immunoprecipitation (co-IP) in *C. elegans*. For all biochemical experiments, we used the PD4251 strain as a control. This strain contains *Pmyo-3*::*gfp* with a mitochondrial localization signal and *Pmyo-3*::*lacZ-gfp* with a nuclear localization signal (Fire et al., 1998). This strain will be referred to as *myo-3*::*gfp*. We prepared lysates from mixed-stage *akt-1*::*gfp; pptr-1*::*mC-flag* and *myo-3*::*gfp; pptr-1*::*mcherry-flag* transgenic worms. Following immunoprecipitation with either anti-FLAG or anti-GFP antibody, we found that PPTR-1 specifically interacts with AKT-1 and not with MYO-3::GFP (Figure 4A; Materials and Methods). We also performed co-IP experiments to investigate whether PPTR-1 and AKT-2 interact, since we observed partial overlap in expression pattern of these proteins. We find that PPTR-1 does not interact with AKT-2 (Supplemental Figure 3). Our epistasis analyses show no genetic interaction between *pptr-1* and *sgk-1*. Moreover, we observe no overlap in the expression pattern of these two proteins using confocal microscopy (Supplemental Movies). However, we find that PPTR-1::mC-FLAG and SGK-1::GFP can interact in our co-IP experiments (Supplemental Figure 3). We do not believe this biochemical interaction to have a measurable functional output and did not pursue it further.

In mammals, Akt is activated by PDK phosphorylation at Thr 308 and PDK-2/TORC-2 protein complex at Ser 473 (Brazil and Hemmings, 2001; Sarbassov et al., 2005). In *C. elegans* AKT-1, these sites correspond to Thr 350 and Ser 517, respectively. We generated affinity-purified phospho-specific antibodies (21st Century BioChemicals, USA; Materials and Methods) against both sites to further investigate the role of PPTR-1 on AKT-1 phosphorylation. Following immunoprecipitation with anti-GFP antibody from either *akt-1*::*gfp* or *akt-1*::*gfp;pptr-1*::*mC-flag* strain, we compared the phosphorylation status at these two sites. We find that overexpressing PPTR-1 can dramatically decrease the phosphorylation of the T350 site while having a marginal effect on the Ser 517 site (Figure 4B). As a control experiment, we treated the immunoprecipitated AKT-1::GFP samples with lambda phosphatase and observed loss of the Thr and Ser phosphorylation, showing the specificity of the phospho-AKT antibodies (Supplemental Figure 4A). Thus, in *C. elegans*, PPTR-1 functions by directly regulating the dephosphorylation of AKT-1 primarily at the Thr 350 (mammalian Thr 308) site.

Mammalian PPTR-1 homolog regulates AKT-1 phosphorylation

Given the evolutionary conservation of the *C. elegans* IIS pathway, we next determined if this mechanism of AKT-1 dephosphorylation mediated by PPTR-1 is also conserved in mammals. The mammalian B56 family of PP2A regulatory subunits has 8 members encoded by 5 genes that express in different tissues (Eichhorn et al., 2008). We used 3T3-L1 adipocytes to perform these studies since in this system, there is a well-characterized insulin signaling pathway that is responsive to changes in insulin levels (Ugi et al., 2004; Watson et al., 2004). We first compared microarray data from the expression profiles of fibroblasts to differentiated 3T3-L1 adipocytes (Powelka et al., 2006) to determine which B56 members were expressed in the adipocytes. We identified 2 genes, PPP2R5A (B56α) and PPP2R5B (B56β) as the top candidates. We knocked down either one or both these regulatory subunits by designing Smartpool siRNAs (Dharmacon, USA) and verified the silencing by quantitative RT PCR (Supplemental Figure 3B). Serum-starved siRNA-treated 3T3-L1 adipocytes were then stimulated with increasing concentrations of insulin. The cells were lysed and the proteins analyzed by western blotting using mammalian Akt phospho-specific antibodies (Materials

and Methods). Knockdown of B56β results in a dramatic increase in phosphorylation at the Thr 308 site of Akt with relatively less changes in Ser 473 phosphorylation (Figure 4C). However, silencing of B56α had no effect on the phosphorylation status of Akt at either site. We observed that siRNA against both the PP2A catalytic subunits (PP2Acα/β) results in increased phosphorylation at Thr 308 but not at Ser 473. Together, our data suggests that PPTR-1/B56β regulatory subunits function to modulate AKT-1 phosphorylation in a conserved manner across phylogeny.

PPTR-1 positively regulates DAF-16 nuclear localization and activity

DAF-16 nuclear localization—We next determined the consequences of modulating PPTR-1 dosage on the IIS pathway. In *C. elegans*, one of the major targets of AKT-1 is the forkhead transcription factor, DAF-16. Active signaling through the IIS pathway results in the phosphorylation of DAF-16 by AKT-1, AKT-2 and SGK-1, leading to its nuclear exclusion (Antebi, 2007; Kenyon, 2005; Wolff and Dillin, 2006). However, under low signaling conditions, DAF-16 translocates into the nucleus, where it can directly bind and activate/repress the transcription of target genes involved in dauer formation, lifespan, stress resistance and fat storage (Oh et al., 2006). We asked whether *pptr-1* regulates IIS pathway-specific phenotypes by modulating DAF-16 function. Since we observed reduced phosphorylation of AKT-1 upon overexpression of PPTR-1, we first looked at the effect of PPTR-1 overexpression on DAF-16 nuclear localization (Henderson and Johnson, 2001; Lee et al., 2001; Lin et al., 2001). We generated a *daf-16*::*gfp;pptr-1*::*mC-flag* strain and then compared the DAF-16 nuclear localization in these worms with a *daf-16*::*gfp* strain (Figure 5A and Supplemental Figure 5A). We categorized DAF-16::GFP localization as completely cytosolic, mostly cytosolic, mostly nuclear or completely nuclear. We find that DAF-16::GFP nuclear localization is enhanced when PPTR-1 is overexpressed (Figure 5A and Supplemental Figure 5A). To determine the specificity of this response, we used *mCherry* RNAi to effectively knockdown *mCherry* expression in *pptr-1*::*mC-flag* thereby reducing the expression of *pptr-1* transgene (data not shown). Our results show that the enhanced nuclear localization upon PPTR-1 overexpression is suppressed when *pptr-1*::*mC-flag;daf-16*::*gfp* worms are grown on *mCherry* RNAi (Figure 5A and Supplemental Figure 5A) and *mCherry* RNAi has little effect on DAF-16 localization in *daf-16*::*gfp* worms. These experiments suggest that increased dosage of *pptr-1* affects DAF-16 nuclear localization. Consistent with its role in the *C. elegans* IIS pathway, we find that overexpression of *pptr-1* significantly increases the lifespan of wild type worms but does not further enhance the lifespan *daf-2(e1370)* worms (Figure 5B and Supplemental Table 3B; mean lifespan of wild type is 23.9 ± 0.3 days, *pptr-1*::*mC-flag* is 30.1 ± 0.5 days, p<.0001, and the *unc-119(+); unc-119(ed3)* control strain is 22.6 ± 0.3 days).

As a corollary to this experiment, we next looked at the effect of *pptr-1*RNAi on DAF-16 nuclear localization. For this, we generated a strain with a *daf-2(e1370);daf-16*::*gfp* strain. At the permissive temperature of 15°C, DAF-16::GFP is excluded from the nucleus in the *daf-2(e1370);daf-16*::*gfp* strain. However, at the non-permissive temperature of 25 °C, progressive nuclear localization of DAF-16::GFP is observed. We grew *daf-2(e1370);daf-16*::*gfp* worms on either vector, *pptr-1* or *daf-18* RNAi and measured the extent of nuclear localization at 25 °C. We find that *pptr*-1 RNAi significantly reduced DAF-16 nuclear localization, similar to the effect of *daf-18* RNAi (Figure 5C and Supplemental Figure 5B). Together, these experiments suggest that changes in PPTR-1 levels affect the activity of AKT-1 and as a result, modulate DAF-16 sub-cellular localization.

DAF-16 target genes—DAF-16 regulates the transcription of many downstream genes such as *sod-3*, *hsp-12.6*, *sip-1* and *mtl-1* (Furuyama et al., 2000; Lee et al., 2003; McElwee et al., 2003; Murphy et al., 2003; Oh et al., 2006). We next tested the effects of *pptr-1* RNAi on these

DAF-16 transcriptional targets. We first tested *sod-3* which has been shown to be a direct target of DAF-16 by chromatin immunoprecipitation (Oh et al., 2006) and its expression changes in response to modulation of the IIS pathway (Furuyama et al., 2000; Libina et al., 2003; Murphy et al., 2003). We grew a *daf-2(e1370);Psod-3::gfp(muIs84)* strain on either vector, *daf-18* or *pptr-1* RNAi to look at the effect on GFP expression. Similar to worms grown on *daf-18* RNAi, *pptr-1* RNAi reduces expression of GFP (Figure 5D and Supplemental Figure 5C). Therefore, modulation in the levels of *pptr-1* can affect the expression of direct DAF-16 target genes.

We further analyzed the expression of known DAF-16 target genes by quantitative RT-PCR in a *daf-2(e1370)* mutant background. As a control, we analyzed whether each of these target genes expressed in a *daf-16*-dependent manner as previously reported (McElwee et al., 2003; Murphy et al., 2003; Oh et al., 2006). As shown in Figure 5E and Supplemental Figure 5D, *daf-16* RNAi dramatically suppressed the expression levels of these genes. Next, we tested the effects of either *pptr-1* or *daf-18* RNAi on the expression of these genes. We found that *pptr-1* RNAi also suppressed the expression of these genes to a level similar to *daf-18* RNAi. Taken together, our data suggests that PPTR-1 positively regulates DAF-16 nuclear localization and thereby its activity.

Discussion

In a directed RNAi screen for Ser/Thr phosphatases in the *C. elegans* IIS pathway, we identified *pptr-1*, a B6 regulatory subunit of the PP2A holoenzyme. PP2A itself is a ubiquitously expressed phosphatase that is involved in multiple cellular processes including regulation of insulin signaling by direct dephosphorylation of Akt (Andjelkovic et al., 1996; Resjo et al., 2002; Ugi et al., 2004). Substrate specificity of PP2A is achieved by its association with distinct regulatory subunits. Our studies provide a mechanistic insight into how the *C. elegans* PP2A regulatory subunit PPTR-1 modulates insulin signaling by specifically regulating AKT-1 phosphorylation and activity in the context of a whole organism.

In our model (Figure 5F), PPTR-1 acts to negatively regulate signals transduced through the IIS pathway, ultimately controlling the activity of the FOXO transcription factor DAF-16. Under low signaling conditions, DAF-16 is able to translocate to the nucleus and transactivate or repress its downstream targets. It is well established that AKT modulates DAF-16 sub-cellular localization. Thus, the activity of AKT-1, as governed by its phosphorylation status, directly translates into the activity of DAF-16. In this study, we show that PPTR-1 directly interacts with AKT-1 and regulates its activity by modulating its phosphorylation, predominantly at the Thr 350 site. Less active AKT-1 results in increased DAF-16 nuclear localization. Indeed, DAF-16 is found to be more nuclear throughout the worm when PPTR-1 is overexpressed. As a corollary, knocking down *pptr-1* by RNAi results in less nuclear DAF-16 as well as reduced expression of DAF-16 target genes such as *sod-3*, *hsp-12.6*, *mtl-1* and *sip-1*. These genes are known to play a combinatorial role in adaptation to various stresses, leading to enhanced dauer formation and increased lifespan. Consistent with the decreased levels of these important genes, *pptr-1* RNAi results in a significant decrease in the dauer formation, lifespan, thermotolerance of *daf-2(e1370)* mutants. In addition, *pptr-1* also regulates other DAF-16-dependent outputs of the IIS pathway such as fat storage. Thus, we find that normal levels of *pptr-1* are important under low insulin signaling conditions. However, *pptr-1* RNAi does not affect IIS pathway-associated phenotypes in wild type worms. There could be several reasons for this observation. Firstly, under normal signaling conditions, AKT-1, AKT-2 as well as SGK-1 are active and negatively regulate DAF-16. Therefore, changes in the AKT-1 activity alone brought about by *pptr-1* RNAi may not have a significant effect on DAF-16-dependent phenotypes. Secondly, PPTR-1 itself may be negatively regulated by the IIS pathway, leading to increased AKT-1 phosphorylation. Along similar lines, in mammals, insulin signaling can downregulate the expression and activity of the PP2A catalytic

subunit (Hojlund et al., 2002; Srinivasan and Begum, 1994; Ugi et al., 2004). Thus, under normal conditions, further down regulation of *pptr-1* by RNAi may have no effect. We speculate that in *C elegans*, in response to changing environmental cues, PPTR-1 helps to downregulate the insulin signaling pathway to promote DAF-16 activity, enabling the worm to either enter diapause or enhance its tolerance to stress as adults.

In mammals, Akt controls a myriad of secondary signaling cascades that regulate glucose transport, protein synthesis, genomic stability, cell survival and gene expression (Toker and Yoeli-Lerner, 2006). Previous studies have implicated roles for PP2A and PHLPP phosphatases in the negative regulation of Akt (Kuo et al., 2008). The PP2A inhibitor Okadaic acid can increase Akt phosphorylation predominantly at Thr 308 and enhance glucose transport in adipocytes (Rondinone et al., 1999). Consistent with this, our results show that siRNA knockdown of the PP2A catalytic subunit and more importantly, the B56β regulatory subunit results in enhanced Akt phosphorylation at Thr 308 in 3T3-L1 adipocytes. Thus, our study points at the remarkable functional conservation of the B56/PPTR-1 regulatory subunit of PP2A in regulating AKT phosphorylation between *C. elegans* and higher mammals. In worms, we also see a modest effect on Ser 517 (equivalent to mammalian Ser 473) phosphorylation by PPTR-1 overexpression. However, we do not observe a difference in Ser 473 phosphorylation in adipocytes. This difference may be explained by the fact that in worms, we are determining the phosphorylation of AKT-1 in the context of a whole organism. Additionally, in mammals phosphorylation state of one Akt site may influence the status of the other (Gao et al., 2005; Toker and Newton, 2000). We do not see a role for the PP2A B55 subunit (*sur-6*) in the *C. elegans* IIS pathway. However, a recent report using cell culture has implicated the mammalian B55 in the regulation of AKT (Kuo et al., 2008).

Dysregulation of Akt has been implicated in diseases such as cancer and diabetes (Rondinone et al., 1999; Sasaoka et al., 2006; Smith et al., 1999; Zdychova and Komers, 2005). In fact, the onset of diabetes is often associated with changes in Akt phosphorylation (Zdychova and Komers, 2005). In several cancer models, loss of function mutations in the PTEN results in hyper-phosphorylated and activated Akt (Groszer et al., 2001; Hakem and Mak, 2001; Stiles et al., 2002; Testa and Bellacosa, 2001) Our studies show that like PTEN, PPTR-1 acts to negatively regulate the insulin/IGF-1 signaling. Given the important role of PPTR-1/B56 in modulating Akt activity, this protein may be a potential therapeutic target for the treatment of diabetes as well as cancer.

Materials and Methods

Strains

All strains were maintained at 15°C using standard *C. elegans* techniques (Stiernagle, 2006). Double mutants were made using standard genetic methods while transgenic worms were made by microparticle bombardment as described in the Supplemental Materials and Methods. For all RNAi assays, the worms were grown for at least two full generations on the RNAi bacteria. Preparation of RNAi plates is described in the Supplemental Materials and Methods.

C. elegans assays

C. elegans assays were modified from previously published methods (Henderson and Johnson, 2001; Kimura et al., 1997; Libina et al., 2003; Oh et al., 2006; Oh et al., 2005). For detailed description of these assays see Supplemental Materials and Methods.

C. elegans immunoprecipitation (IP) and western blotting

Transgenic worms were grown in three 100 mm plates seeded with OP50 bacteria at 20 °C. Worms were harvested by washing with M9 buffer and pellet collected by centrifugation. The

pellet was resuspended in 250 μl lysis buffer (20 mM Tris-Cl, 137 mM NaCl, 10% glycerol, 1% Triton X-100, 25 mM β-glycerophosphate, Protease inhibitor cocktail (Roche Biochemicals, USA), pH 7.4). The worms were sonicated with Bioruptor (Diagenode, USA) using maximum power output (1 min sonication, 2 min off-repeated 10 times). The lysate was cleared by centrifugation and protein content estimated by Bradford method. Lysate equivalent to 1.5 mg total protein was pre-cleared with 50 μl of protein-G agarose beads, fast flow (Upstate, USA) and then immunoprecipitated overnight at 4 °C using either anti-GFP monoclonal antibody (Sigma, USA) or anti-FLAG M2 gel (Sigma, USA). The following morning, 50 μl protein-G agarose beads, fast flow were added to the GFP IP to capture the immune complex. The agarose beads were then washed 5 times with lysis buffer. Following this step, the beads were boiled in Laemelli's buffer.

For western blot analysis, immunoprecipitated protein samples was resolved on a 10% SDS-PAGE and transferred to nitrocellulose membranes. Membranes were blocked in TBST (Tris Buffered Saline containing 0.05% Tween 20, ph 7.4) containing 5% non-fat milk at RT for 1 hour. Membranes were then washed with TBST and incubated overnight with 1:1000 dilutions of antibodies in TBST containing 5% non-fat milk 4 °C. Membranes were washed 3 times with TBST and then incubated with TBST containing 5% non-fat milk containing a 1:10,000 dilution of the secondary antibody. Antibodies used for western were:

Living Color DsRed antibody (Clontech, USA; Catalog no. 632496)

Living Color Rabbit polyclonal GFP antibody (BD Biosciences, USA; Catalog no. 632460)

Monoclonal mAb 3e6 GFP antibody (Invitrogen, USA; Catalog no. A11120)

Anti-FLAG M2 Affinity Gel (Sigma, USA; Catalog no. A2220).

C. elegans phospho-AKT western blotting

Transgenic worms were grown at 20 °C in 3-4 large (100 mm) plates seeded with OP50. Worms were collected by washing with 1 X PBS and the pellet was then immediately frozen in dry ice. Around 500 μl lysis buffer, supplemented by Sigma Phosphatase inhibitor cocktails I and II (50×) and Protease inhibitor cocktail (Roche Biochemicals, USA) was added to the pellet and sonicated using a Misonix (3000) sonicator (Misonix, USA; power output set at 4, 3 pulses of 10 secs each with 1 min interval between pulses). The lysates were clarified by centrifugation at 13000 rpm for 10 mins at 4°C and the protein content estimated by Quick Bradford (Pierce). About 3.5 μg of anti-GFP monoclonal antibody (3E6, Invitrogen USA) was used for each IP from lysates containing 1.7 mg protein in a volume of 1ml. IPs were performed overnight at 4°C and antibody-protein complexes were captured using 50 μl of protein-G agarose beads, fast flow (Upstate, USA) for 2 hrs at 4°C. The pellets were washed 3 times with lysis buffer supplemented by protease and phosphatase inhibitors and boiled in Laemelli's buffer. The IP samples were then resolved on a 10% SDS-PAGE, western blotted and analyzed with phospho-specific antibodies (Supplemental Materials and Methods).

Mammalian cell culture and phosphor-Akt Western blotting

3T3-L1 adipocytes were cultured and differentiated as previously described (Tesz et al., 2007). For siRNA transfections, cells from 4 days post-induction of adipocyte differentiation were used as previously described (Tang et al., 2006). Cells were stimulated with increasing concentrations of insulin and isolated proteins were analyzed by Western blotting Detailed procedure is described in Supplemental Materials and Methods.

RNA isolation and real-time PCR

Total RNA was isolated using Trizol (Invitrogen, USA) and real-time PCR was performed according to manufacturer's instructions (Applied Biosystems, USA) as detailed in Supplemental Materials and Methods.

Supplementary Material

Refer to Web version on PubMed Central for supplementary material.

Acknowledgments

We are grateful to Eun-soo Kwon, Kelvin Yen, Craig Mello and Marian Walhout for advice and critical comments on the manuscript, Paul Furcinitti of the UMass Medical School Digital Light Microscopy Core Facility for help with the confocal microscopy, Nina Bhabhalia for technical support and Sandhya Pande for help with the phospho-westerns. We thank Marian Walhout, Gary Ruvkun, Maren Hertweck and Ralf Baumeister for plasmids and strains. Some of the strains were kindly provided by Theresa Stiernagle at the *Caenorhabditis* Genetics Center, which is funded by the National Institutes of Health National Center for Research Resources. H.A.T. is a William Randolph Hearst Young Investigator. This project was funded in part by NIA (AG025891), the Glenn Foundation an endowment from the William Randolph Hearst Foundation.

References

Andjelkovic M, Jakubowicz T, Cron P, Ming XF, Han JW, Hemmings BA. Activation and phosphorylation of a pleckstrin homology domain containing protein kinase (RAC-PK/PKB) promoted by serum and protein phosphatase inhibitors. Proc Natl Acad Sci U S A 1996;93:5699–5704. [PubMed: 8650155]

Antebi A. Genetics of aging in *Caenorhabditis elegans*. PLoS Genet 2007;3:1565–1571. [PubMed: 17907808]

Ashrafi K, Chang FY, Watts JL, Fraser AG, Kamath RS, Ahringer J, Ruvkun G. Genome-wide RNAi analysis of *Caenorhabditis elegans* fat regulatory genes. Nature 2003;421:268–272. [PubMed: 12529643]

Barbieri M, Bonafe M, Franceschi C, Paolisso G. Insulin/IGF-I-signaling pathway: an evolutionarily conserved mechanism of longevity from yeast to humans. Am J Physiol Endocrinol Metab 2003;285:E1064–1071. [PubMed: 14534077]

Brazil DP, Hemmings BA. Ten years of protein kinase B signalling: a hard Akt to follow. Trends Biochem Sci 2001;26:657–664. [PubMed: 11701324]

Brunet A, Bonni A, Zigmond MJ, Lin MZ, Juo P, Hu LS, Anderson MJ, Arden KC, Blenis J, Greenberg ME. Akt promotes cell survival by phosphorylating and inhibiting a Forkhead transcription factor. Cell 1999;96:857–868. [PubMed: 10102273]

Brunet A, Park J, Tran H, Hu LS, Hemmings BA, Greenberg ME. Protein kinase SGK mediates survival signals by phosphorylating the forkhead transcription factor FKHRL1 (FOXO3a). Mol Cell Biol 2001;21:952–965. [PubMed: 11154281]

da Graca LS, Zimmerman KK, Mitchell MC, Kozhan-Gorodetska M, Sekiewicz K, Morales Y, Patterson GI. DAF-5 is a Ski oncoprotein homolog that functions in a neuronal TGF beta pathway to regulate *C. elegans* dauer development. Development 2004;131:435–446. [PubMed: 14681186]

Dorman JB, Albinder B, Shroyer T, Kenyon C. The *age-1* and *daf-2* Genes Function in a Common Pathway to Control the Lifespan of *Caenorhabditis elegans*. Genetics 1995;141:1399–1406. [PubMed: 8601482]

Eichhorn PJ, Creyghton MP, Bernards R. Protein phosphatase 2A regulatory subunits and cancer. Biochim Biophys Acta. 2008

Fire A, Xu S, Montgomery MK, Kostas SA, Driver SE, Mello CC. Potent and specific genetic interference by double-stranded RNA in *Caenorhabditis elegans*. Nature 1998;391:806–811. [PubMed: 9486653]

Furuyama T, Nakazawa T, Nakano I, Mori N. Identification of the differential distribution patterns of mRNAs and consensus binding sequences for mouse DAF-16 homologues. Biochem J 2000;349:629–634. [PubMed: 10880363]

Gao T, Furnari F, Newton AC. PHLPP: a phosphatase that directly dephosphorylates Akt, promotes apoptosis, and suppresses tumor growth. Mol Cell 2005;18:13–24. [PubMed: 15808505]

Gems D, Sutton AJ, Sundermeyer ML, Albert PS, King KV, Edgley ML, Larsen PL, Riddle DL. Two pleiotropic classes of *daf-2* mutation affect larval arrest, adult behavior, reproduction and longevity in *Caenorhabditis elegans*. Genetics 1998;150:129–155. [PubMed: 9725835]

Gil EB, Malone Link E, Liu LX, Johnson CD, Lees JA. Regulation of the insulin-like developmental pathway of *Caenorhabditis elegans* by a homolog of the PTEN tumor suppressor gene. Proc Natl Acad Sci U S A 1999;96:2925–2930. [PubMed: 10077613]

Groszer M, Erickson R, Scripture-Adams DD, Lesche R, Trumpp A, Zack JA, Kornblum HI, Liu X, Wu H. Negative regulation of neural stem/progenitor cell proliferation by the Pten tumor suppressor gene in vivo. Science 2001;294:2186–2189. [PubMed: 11691952]

Gunther CV, Georgi LL, Riddle DL. A *Caenorhabditis elegans* type I TGF beta receptor can function in the absence of type II kinase to promote larval development. Development 2000;127:3337–3347. [PubMed: 10887089]

Hakem R, Mak TW. Animal models of tumor-suppressor genes. Annu Rev Genet 2001;35:209–241. [PubMed: 11700283]

Henderson ST, Johnson TE. *daf-16* integrates developmental and environmental inputs to mediate aging in the nematode *Caenorhabditis elegans*. Curr Biol 2001;11:1975–1980. [PubMed: 11747825]

Hertweck M, Gobel C, Baumeister R. *C. elegans* SGK-1 is the critical component in the Akt/PKB kinase complex to control stress response and life span. Dev Cell 2004;6:577–588. [PubMed: 15068796]

Hojlund K, Poulsen M, Staehr P, Brusgaard K, Beck-Nielsen H. Effect of insulin on protein phosphatase 2A expression in muscle in type 2 diabetes. Eur J Clin Invest 2002;32:918–923. [PubMed: 12534451]

Honda Y, Honda S. The *daf-2* gene network for longevity regulates oxidative stress resistance and Mn-superoxide dismutase gene expression in *Caenorhabditis elegans*. FASEB J 1999;13:1385–1393. [PubMed: 10428762]

Inoue T, Thomas JH. Targets of TGF-beta signaling in *Caenorhabditis elegans* dauer formation. Developmental Biology 2000;217:192–204. [PubMed: 10625546]

Janssens V, Longin S, Goris J. PP2A holoenzyme assembly: in cauda venenum (the sting is in the tail). Trends Biochem Sci 2008;33:113–121. [PubMed: 18291659]

Jensen VL, Albert PS, Riddle DL. *Caenorhabditis elegans* SDF-9 enhances insulin/insulin-like signaling through interaction with DAF-2. Genetics 2007;177:661–666. [PubMed: 17660545]

Kamath RS, Fraser AG, Dong Y, Poulin G, Durbin R, Gotta M, Kanapin A, Le Bot N, Moreno S, Sohrmann M, et al. Systematic functional analysis of the *Caenorhabditis elegans* genome using RNAi. Nature 2003;421:231–237. [PubMed: 12529635]

Kenyon C. The plasticity of aging: insights from long-lived mutants. Cell 2005;120:449–460. [PubMed: 15734678]

Kenyon C, Chang J, Gensch E, Rudner A, Tabtiang R. A *C. elegans* mutant that lives twice as long as wild type. Nature 1993;366:461–464. [PubMed: 8247153]

Kimble J, Edgar L, Hirsh D. Specification of male development in *Caenorhabditis elegans*: the fem genes. Dev Biol 1984;105:234–239. [PubMed: 6468762]

Kimura KD, Tissenbaum HA, Liu Y, Ruvkun G. *daf-2*, an insulin receptor-like gene that regulates longevity and diapause in *Caenorhabditis elegans*. Science 1997;277:942–946. [PubMed: 9252323]

Kuo YC, Huang KY, Yang CH, Yang YS, Lee WY, Chiang CW. Regulation of phosphorylation of Thr-308 of Akt, cell proliferation, and survival by the B55alpha regulatory subunit targeting of the protein phosphatase 2A holoenzyme to Akt. J Biol Chem 2008;283:1882–1892. [PubMed: 18042541]

Larsen PL, Albert PS, Riddle DL. Genes that regulate both development and longevity in *Caenorhabditis elegans*. Genetics 1995;139:1567–1583. [PubMed: 7789761]

Lee RY, Hench J, Ruvkun G. Regulation of *C. elegans* DAF-16 and its human ortholog FKHRL1 by the *daf-2* insulin-like signaling pathway. Curr Biol 2001;11:1950–1957. [PubMed: 11747821]

Lee SS, Kennedy S, Tolonen AC, Ruvkun G. DAF-16 target genes that control *C. elegans* life-span and metabolism. Science 2003;300:644–647. [PubMed: 12690206]

Libina N, Berman JR, Kenyon C. Tissue-specific activities of *C. elegans* DAF-16 in the regulation of lifespan. Cell 2003;115:489–502. [PubMed: 14622602]

Lin K, Dorman JB, Rodan A, Kenyon C. *daf-16*: An HNF-3/forkhead family member that can function to double the life-span of *Caenorhabditis elegans*. Science 1997;278:1319–1322. [PubMed: 9360933]

Lin K, Hsin H, Libina N, Kenyon C. Regulation of the *Caenorhabditis elegans* longevity protein DAF-16 by insulin/IGF-1 and germline signaling. Nat Genet 2001;28:139–145. [PubMed: 11381260]

Lithgow GJ, Walker GA. Stress resistance as a determinate of *C. elegans* lifespan. Mech Ageing Dev 2002;123:765–771. [PubMed: 11869734]

Lithgow GJ, White TM, Melov S, Johnson TE. Thermotolerance and extended life-span conferred by single-gene mutations and induced by thermal stress. Proc Natl Acad Sci U S A 1995;92:7540–7544. [PubMed: 7638227]

McElwee J, Bubb K, Thomas JH. Transcriptional outputs of the *Caenorhabditis elegans* forkhead protein DAF-16. Aging Cell 2003;2:111–121. [PubMed: 12882324]

Mihaylova VT, Borland CZ, Manjarrez L, Stern MJ, Sun H. The PTEN tumor suppressor homolog in *Caenorhabditis elegans* regulates longevity and dauer formation in an insulin receptor-like signaling pathway. Proc Natl Acad Sci U S A 1999;96:7427–7432. [PubMed: 10377431]

Morris JZ, Tissenbaum HA, Ruvkun G. A phosphatidylinositol-3-OH kinase family member regulating longevity and diapause in *Caenorhabditis elegans*. Nature 1996;382:536–539. [PubMed: 8700226]

Mukhopadhyay A, Oh SW, Tissenbaum HA. Worming pathways to and from DAF-16/FOXO. Exp Gerontol 2006;41:928–934. [PubMed: 16839734]

Munoz MJ, Riddle DL. Positive selection of *Caenorhabditis elegans* mutants with increased stress resistance and longevity. Genetics 2003;163:171–180. [PubMed: 12586705]

Murphy CT, McCarroll SA, Bargmann CI, Fraser A, Kamath RS, Ahringer J, Li H, Kenyon C. Genes that act downstream of DAF-16 to influence the lifespan of *Caenorhabditis elegans*. Nature 2003;424:277–283. [PubMed: 12845331]

Ogg S, Paradis S, Gottlieb S, Patterson GI, Lee L, Tissenbaum HA, Ruvkun G. The Fork head transcription factor DAF-16 transduces insulin-like metabolic and longevity signals in *C. elegans*. Nature 1997;389:994–999. [PubMed: 9353126]

Ogg S, Ruvkun G. The *C. elegans* PTEN homolog, DAF-18, acts in the insulin receptor-like metabolic signaling pathway. Molecular Cell 1998;2:887–893. [PubMed: 9885576]

Oh SW, Mukhopadhyay A, Dixit BL, Raha T, Green MR, Tissenbaum HA. Identification of direct DAF-16 targets controlling longevity, metabolism and diapause by chromatin immunoprecipitation. Nat Genet 2006;38:251–257. [PubMed: 16380712]

Oh SW, Mukhopadhyay A, Svrzikapa N, Jiang F, Davis RJ, Tissenbaum HA. JNK regulates lifespan in *Caenorhabditis elegans* by modulating nuclear translocation of forkhead transcription factor/DAF-16. Proc Natl Acad Sci U S A 2005;102:4494–4499. [PubMed: 15767565]

Paradis S, Ailion M, Toker A, Thomas JH, Ruvkun G. A PDK1 homolog is necessary and sufficient to transduce AGE-1 PI3 kinase signals that regulate diapause in *Caenorhabditis elegans*. Genes Dev 1999;13:1438–1452. [PubMed: 10364160]

Paradis S, Ruvkun G. *Caenorhabditis elegans* Akt/PKB transduces insulin receptor-like signals from AGE-1 PI3 kinase to the DAF-16 transcription factor. Genes Dev 1998;12:2488–2498. [PubMed: 9716402]

Patterson GI, Koweek A, Wong A, Liu Y, Ruvkun G. The DAF-3 Smad protein antagonizes TGF-beta-related receptor signaling in the *Caenorhabditis elegans* dauer pathway. Genes Dev 1997;11:2679–2690. [PubMed: 9334330]

Patterson GI, Padgett RW. TGF beta-related pathways. Roles in *Caenorhabditis elegans* development. Trends Genet 2000;16:27–33. [PubMed: 10637628]

Pilgrim D, McGregor A, Jackle P, Johnson T, Hansen D. The *C. elegans* sex-determining gene *fem-2* encodes a putative protein phosphatase. Mol Biol Cell 1995;6:1159–1171. [PubMed: 8534913]

Powelka AM, Seth A, Virbasius JV, Kiskinis E, Nicoloro SM, Guilherme A, Tang X, Straubhaar J, Cherniack AD, Parker MG, Czech MP. Suppression of oxidative metabolism and mitochondrial biogenesis by the transcriptional corepressor RIP140 in mouse adipocytes. J Clin Invest 2006;116:125–136. [PubMed: 16374519]

Reboul J, Vaglio P, Rual JF, Lamesch P, Martinez M, Armstrong CM, Li S, Jacotot L, Bertin N, Janky R, et al. *C. elegans* ORFeome version 1.1: experimental verification of the genome annotation and resource for proteome-scale protein expression. Nat Genet 2003;34:35–41. [PubMed: 12679813]

Ren P, Lim C, Johnsen R, Albert PS, Pilgrim D, Riddle DL. Control of *C. elegans* Larval Development by Neuronal Expression of a TGF-β homologue. Science 1996;274:1389–1391. [PubMed: 8910282]

Resjo S, Goransson O, Harndahl L, Zolnierowicz S, Manganiello V, Degerman E. Protein phosphatase 2A is the main phosphatase involved in the regulation of protein kinase B in rat adipocytes. Cell Signal 2002;14:231–238. [PubMed: 11812651]

Riddle, D.; B, T.; Meyer, B.; Priess, J. C Elegans II. Vol. 1. Cold Spring Harbor: Cold Spring Harbor Press; 1997.

Riddle DL, Swanson MM, Albert PS. Interacting genes in nematode dauer larva formation. Nature 1981;290:668–671. [PubMed: 7219552]

Rondinone CM, Carvalho E, Wesslau C, Smith UP. Impaired glucose transport and protein kinase B activation by insulin, but not okadaic acid, in adipocytes from subjects with Type II diabetes mellitus. Diabetologia 1999;42:819–825. [PubMed: 10440123]

Rouault JP, Kuwabara PE, Sinilnikova OM, Duret L, Thierry-Mieg D, Billaud M. Regulation of dauer larva development in *Caenorhabditis elegans* by *daf-18*, a homologue of the tumour suppressor PTEN. Current Biology 1999;9:329–332. [PubMed: 10209098]

Sarbassov DD, Guertin DA, Ali SM, Sabatini DM. Phosphorylation and regulation of Akt/PKB by the rictor-mTOR complex. Science 2005;307:1098–1101. [PubMed: 15718470]

Sasaoka T, Wada T, Tsuneki H. Lipid phosphatases as a possible therapeutic target in cases of type 2 diabetes and obesity. Pharmacol Ther 2006;112:799–809. [PubMed: 16842857]

Savage-Dunn C. TGF-beta signaling. WormBook 2005:1–12. [PubMed: 18050404]

Smith U, Axelsen M, Carvalho E, Eliasson B, Jansson PA, Wesslau C. Insulin signaling and action in fat cells: associations with insulin resistance and type 2 diabetes. Ann N Y Acad Sci 1999;892:119–126. [PubMed: 10842657]

Srinivasan M, Begum N. Regulation of protein phosphatase 1 and 2A activities by insulin during myogenesis in rat skeletal muscle cells in culture. J Biol Chem 1994;269:12514–12520. [PubMed: 8175660]

Stiernagle T. Maintenance of *C. elegans*. WormBook 2006:1–11. [PubMed: 18050451]

Stiles B, Gilman V, Khanzenzon N, Lesche R, Li A, Qiao R, Liu X, Wu H. Essential role of AKT-1/protein kinase B alpha in PTEN-controlled tumorigenesis. Mol Cell Biol 2002;22:3842–3851. [PubMed: 11997518]

Tang X, Guilherme A, Chakladar A, Powelka AM, Konda S, Virbasius JV, Nicoloro SM, Straubhaar J, Czech MP. An RNA interference-based screen identifies MAP4K4/NIK as a negative regulator of PPARgamma, adipogenesis, and insulin-responsive hexose transport. Proc Natl Acad Sci U S A 2006;103:2087–2092. [PubMed: 16461467]

Testa JR, Bellacosa A. AKT plays a central role in tumorigenesis. Proc Natl Acad Sci U S A 2001;98:10983–10985. [PubMed: 11572954]

Tesz GJ, Guilherme A, Guntur KV, Hubbard AC, Tang X, Chawla A, Czech MP. Tumor necrosis factor alpha (TNFalpha) stimulates Map4k4 expression through TNFalpha receptor 1 signaling to c-Jun and activating transcription factor 2. J Biol Chem 2007;282:19302–19312. [PubMed: 17500068]

Toker A, Newton AC. Akt/protein kinase B is regulated by autophosphorylation at the hypothetical PDK-2 site. J Biol Chem 2000;275:8271–8274. [PubMed: 10722653]

Toker A, Yoeli-Lerner M. Akt signaling and cancer: surviving but not moving on. Cancer Res 2006;66:3963–3966. [PubMed: 16618711]

Ugi S, Imamura T, Maegawa H, Egawa K, Yoshizaki T, Shi K, Obata T, Ebina Y, Kashiwagi A, Olefsky JM. Protein phosphatase 2A negatively regulates insulin's metabolic signaling pathway by inhibiting Akt (protein kinase B) activity in 3T3-L1 adipocytes. Mol Cell Biol 2004;24:8778–8789. [PubMed: 15367694]

Vowels JJ, Thomas JH. Genetic analysis of chemosensory control of dauer formation in *Caenorhabditis elegans*. Genetics 1992;130:105–123. [PubMed: 1732156]

Watson RT, Kanzaki M, Pessin JE. Regulated membrane trafficking of the insulin-responsive glucose transporter 4 in adipocytes. Endocr Rev 2004;25:177–204. [PubMed: 15082519]

Wolff S, Dillin A. The trifecta of aging in *Caenorhabditis elegans*. Exp Gerontol 2006;41:894–903. [PubMed: 16919905]

Wolkow CA, Munoz MJ, Riddle DL, Ruvkun G. Insulin receptor substrate and p55 orthologous adaptor proteins function in the *Caenorhabditis elegans daf-2*/insulin-like signaling pathway. J Biol Chem 2002;277:49591–49597. [PubMed: 12393910]

Zdychova J, Komers R. Emerging role of Akt kinase/protein kinase B signaling in pathophysiology of diabetes and its complications. Physiol Res 2005;54:1–16. [PubMed: 15717836]

A

Phosphatase family	Members	*C. elegans* homologs
PPM	PP2C	10
	PDP	1
PPP	PP1	3
	PP2A	1
	PP2B	1
	PP4	2
	PP5	1
	PP6	1
	PP1 like	40
PP2A regulatory subunits	B55/PR55	1
	B56/PR61	2
	B72/PR72	4

C

Experiment	RNAi	% Dauer ± Std. Dev.	(n)
1	vector	54.4 ± 4.9	285
	daf-18	0.3 ± 0.5	312
	fem-2	0.0 ± 0.0	388
2	vector	17.5 ± 3.7	405
	daf-18	0.0 ± 0.0	395
	pptr-1	1.3 ± 1.6	470

B

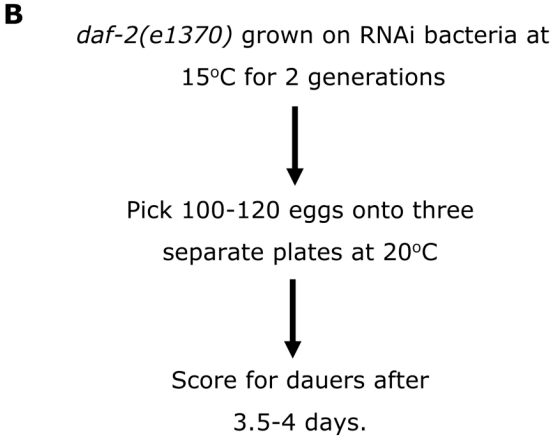

D

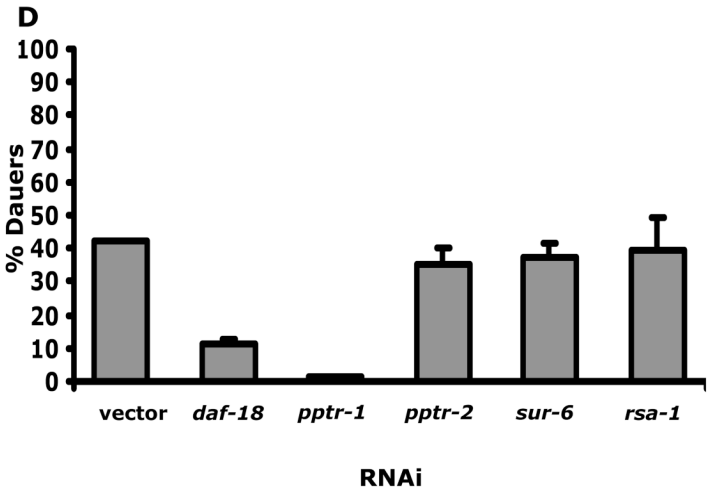

Figure 1.

pptr-1, a regulatory subunit of the PP2A holoenzyme, was identified as a top candidate in a directed RNAi screen to identify serine/threonine phosphatases that regulate the IIS pathway.

A) The different families and classes of the phosphatases included in the RNAi screen.

B) A schematic representation of the RNAi screen. All the assays were performed in triplicate.

C) The top two candidates that dramatically suppressed *daf-2(e1370)* dauer formation at 20° C (*fem-2*, and *pptr-1*). Both *fem-2* and *pptr-1* RNAi were able to suppress *daf-2* dauer formation to a similar level as *daf-18* RNAi. Error bars indicate the standard deviations among the different RNAi plates within one experiment. Data shown [% Dauers ± Std. Dev. (n)] are from one representative experiment.

D) *pptr-1* is the only PP2A regulatory subunit family member that dramatically suppresses *daf-2(1370)* dauer formation. Error bars indicate the standard deviations among the different RNAi plates within one experiment. Data shown are from one representative experiment.

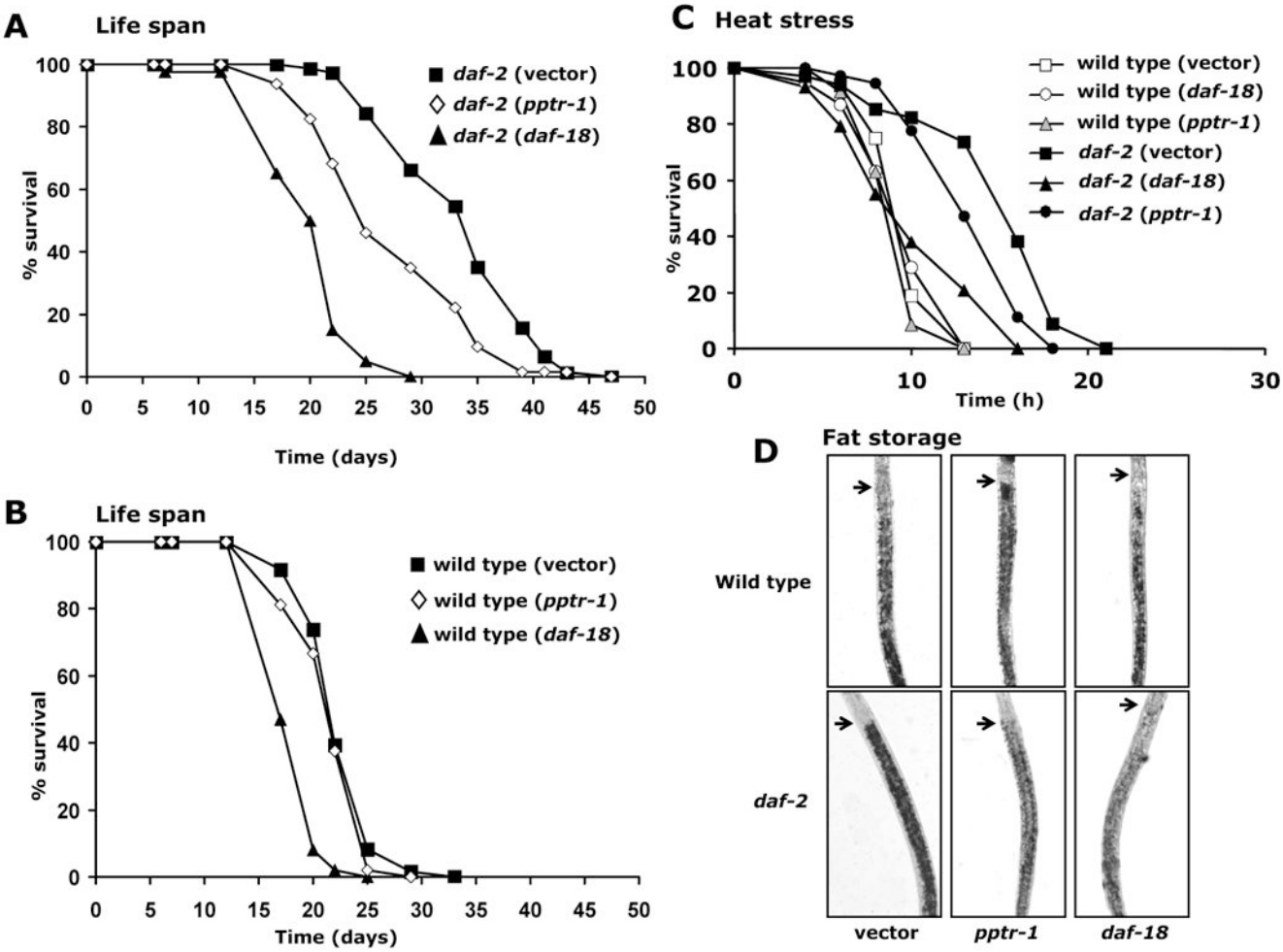

Figure 2.

pptr-1 regulates lifespan, thermotolerance and fat-storage through the IIS pathway. Data shown are from one representative experiment.

A) *pptr-1* RNAi significantly reduces the lifespan of *daf-2(e1370)* mutants similar to *daf-18* RNAi (mean life on vector RNAi is 33.9 ± 0.7 days (n=77), *pptr*-1 RNAi is 27.7 ± 0.9 days (n=63) p <0.0001and on *daf-18* RNAi is 20.4 ± 0.6 days (n=40), p <0.0001)

B) *pptr-1* RNAi does not affect the lifespan of wild-type worms (mean lifespan on vector RNAi is 22.8 ± 0.4 days (n=61), *pptr*-1 RNAi is 21.9 ± 0.5 days (n=49). *daf-18* RNAi reduces mean lifespan of wild type worms to 18.6 ± 0.3 days (n=48) p <0.0001).

C) The thermotolerance of *daf-2(e1370)* worms is reduced by *pptr-1* as well as *daf-18* RNAi (mean survival of *daf-2(e1370)* worms at 37 °C on vector RNAi was 15.2 ± 0.7 hrs (n=34), whereas on *pptr-1* RNAi the survival was 13.8 ± 0.5 hrs (p value< 0.006) (n=36) and 10.3 ± 0.7 hrs (p value< 0.0001) (n=29) on *daf-18* RNAi. *pptr-1* RNAi did not affect the thermotolerance of wild type worms; (mean survival was 9.8 ± 0.4 hrs on vector RNAi (n=32), 9.3 ± 0.3 hrs on *pptr-1* RNAi (n=35) and 9.7 ± 0.4 hrs on *daf-18* RNAi (n=32).

D) Sudan black staining showing that *pptr-1* RNAi reduces the increased fat storage of *daf-2 (e1370)* worms, similar to *daf-18* RNAi but has no effect on wild type fat-storage. Arrows indicate the pharynx. A representative picture from one of three independent experiments (n=30) is shown.

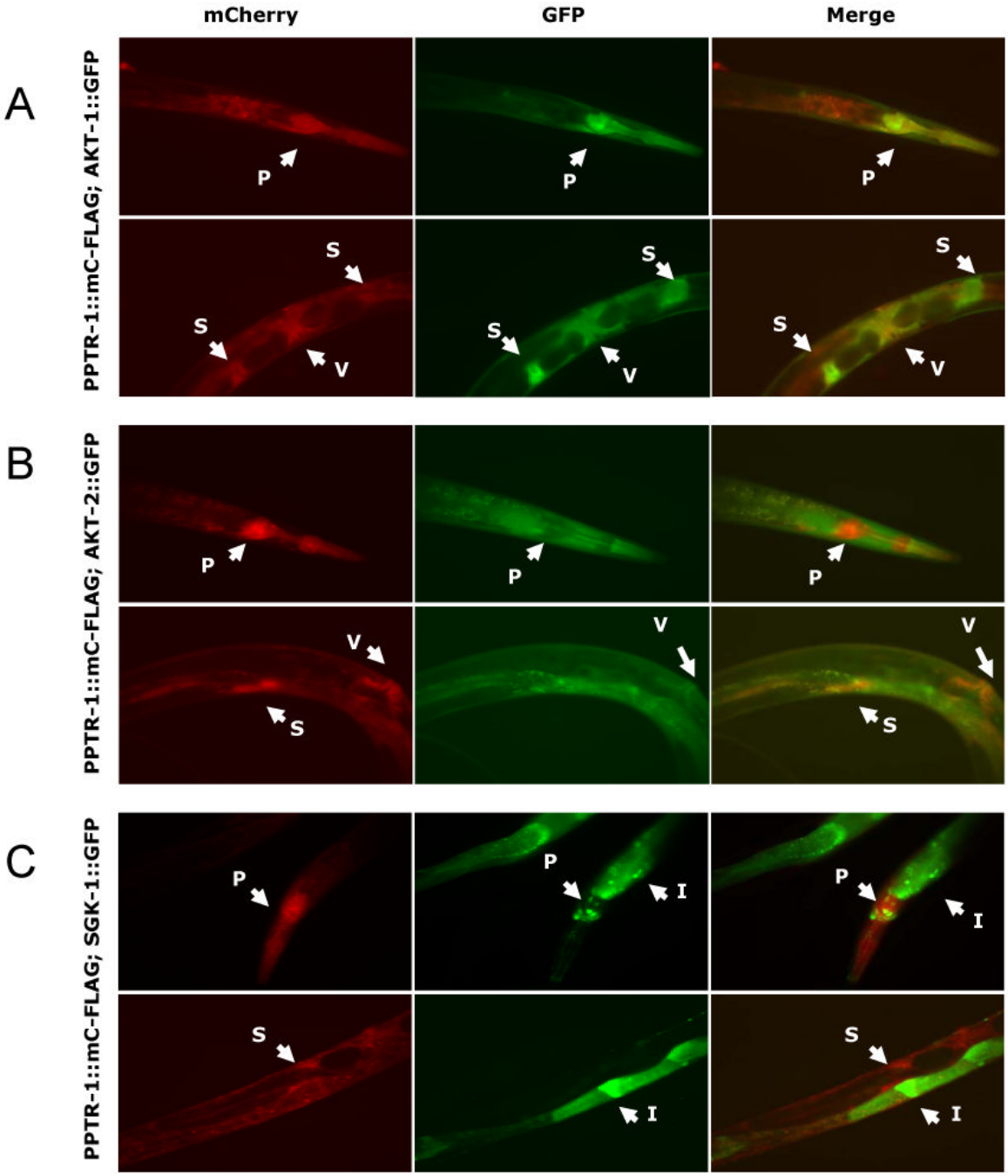

Figure 3.

PPTR-1 co-localizes with AKT-1. *akt-1*::*gfp;pptr-1*::*mC-flag*, *akt-2*::*gfp;pptr-1*::*mC-flag* and *sgk-1*::*gfp;pptr-1*::*mC-flag* transgenic worms were mounted and visualized by fluorescence microscopy using Rhodamine (mCherry) and FITC (GFP) filters. PPTR-1 expression is observed mainly in the pharynx, vulva and spermatheca (A-C, mCherry).

A) Expression of PPTR-1::mC-FLAG (mCherry) and AKT-1::GFP (GFP) in a *akt-1*::*gfp; pptr-1*::*mC-flag* strain. Expression of PPTR-1::mC-FLAG overlaps with AKT-1::GFP (Merge).

B) PPTR-1::mC-FLAG and AKT-2::GFP colocalize in some tissues in a *akt-2*::*gfp; pptr-1*::*mC-flag* strain (Merge).

C) SGK-1::GFP and PPTR-1::mC-FLAG do not colocalize in *sgk-1::gfp;pptr-1::mC-flag* transgenic worms (Merge).
Arrows indicate the following tissues: p-pharynx, v-vulva, s-spermatheca, i-intestine

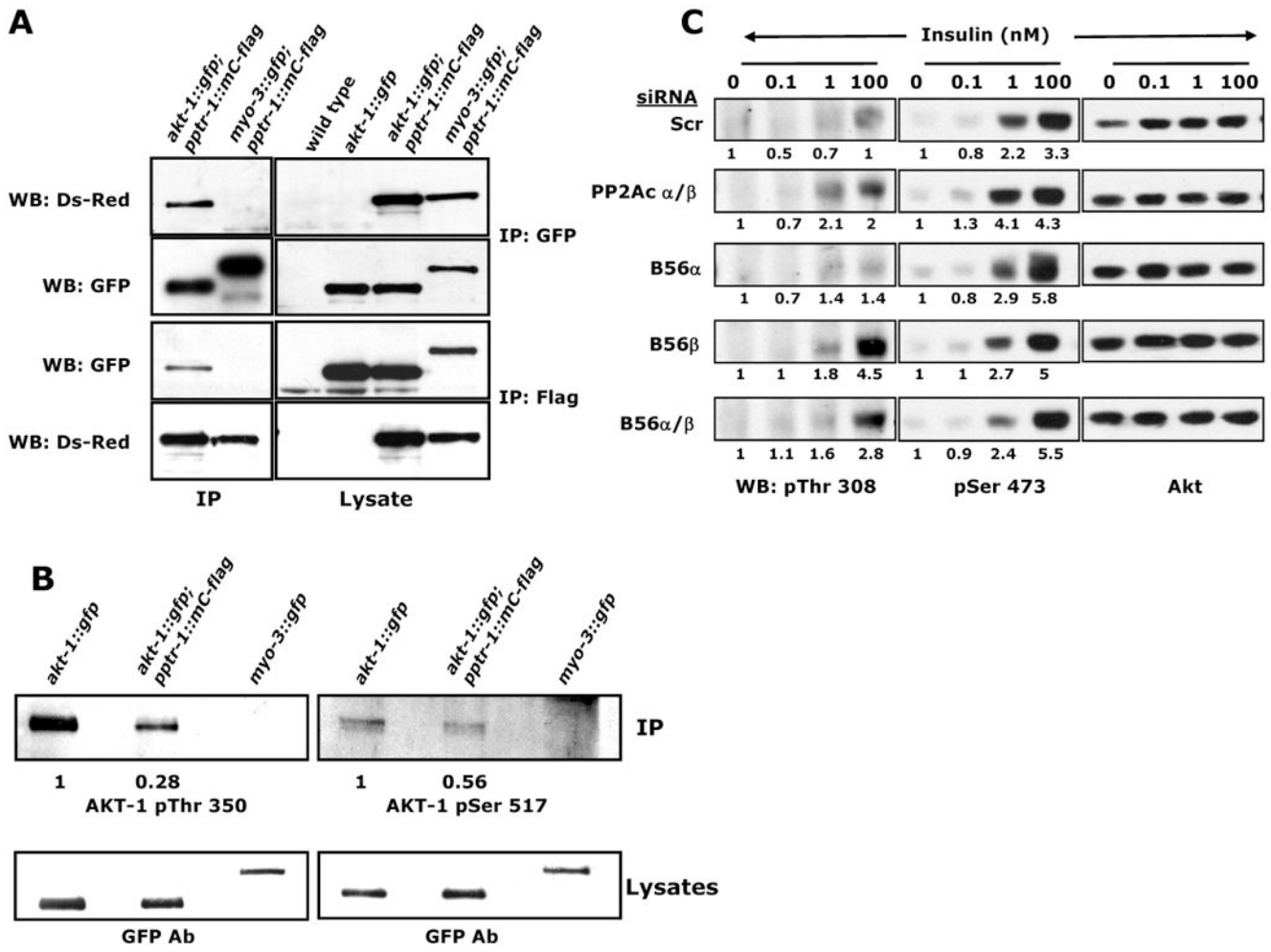

Figure 4.

PPTR-1 interacts with and modulates AKT-1 phosphorylation. Data shown are from one representative experiment

A) PPTR-1 directly interacts with AKT-1 in *C. elegans*. AKT-1::GFP and MYO-3::GFP were immunoprecipated (IP) using anti-GFP antibody and were analyzed by western blotting (WB) using anti-Ds-Red or anti-GFP antibodies. In addition, PPTR-1::mC-FLAG was immunoprecipitated with anti-FLAG antibody and analysed by WB using using anti-Ds-Red or anti-GFP antibodies. Lysates were used for WB analysis.

B) PPTR-1 overexpression reduces AKT-1 phosphorylation in *C. elegans*. AKT-1::GFP and MYO-3::GFP were immunoprecipitated from *akt-1::gfp, akt-1::gfp;pptr-1::mC-flag* and *myo-3::gfp;pptr-1::mC-flag* followed by western blotting using pThr 350 or pSer 517 antibodies (upper panels). Total lysates were analyzed by western blotting (lower panels). Quantification of changes in AKT-1::GFP phosphorylation upon PPTR-1 overexpression is shown below each lane.

C) Knockdown of the mammalian B56β regulatory subunit by siRNA in 3T3-L1 adipocytes increases insulin-stimulated AKT phosphorylation at Thr 308. The 3T3-L1 adipocytes were transfected with scrambled (Scr), PP2Acα/β, B56α, B56 β or B56α/β siRNA. These cells were then treated with increasing concentrations of insulin and phosphorylation status of Akt was analyzed by western blotting using pThr 308 (left) and pSer 473 antibodies (middle). Total Akt

antibody was used as a loading control (right). Quantification of fold changes in Akt phosphorylation is shown below each lane.

A

Strains	RNAi	Completely Cytoplasmic (%)	Mostly Cytoplasmic (%)	Mostly Nuclear (%)	Completely Nuclear (%)	(n)
pptr-1::mC-flag; daf-16::gfp	vector	34.5	22.9	29.6	12.9	77
	mCherry	79.5	18.6	1.95	0	96
daf-16::gfp	vector	50.0	42.5	5.0	2.5	40
	mCherry	55.3	29.8	14.9	0	47

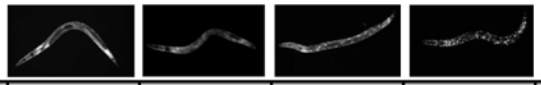

C

Strain	RNAi	Completely Cytoplasmic (%)	Mostly cytoplasmic (%)	Mostly Nuclear (%)	Completely Nuclear (%)	(n)
daf-2(e1370); daf-16::gfp	vector	4.5	40.9	50.0	4.5	22
	daf-18	63.6	45.4	4.5	0	25
	pptr-1	50.0	45.4	4.5	0	22

D

Strain	RNAi	High (%)	Medium (%)	Low (%)	(n)
daf-2(e1370); sod-3::gfp	vector	36.6	46.6	16.6	30
	daf-18	10.0	50.0	40.0	30
	pptr-1	6.6	43.3	50.0	30

E

Strain	RNAi	Transcripts determined by Q-PCR (% of vector RNAi)			
		sod-3	*hsp-12.6*	*sip-1*	*mtl-1*
daf-2(e1370)	*daf-16*	7.8	10.8	24.7	0.7
	daf-18	46.8	35.2	84.1	17.8
	pptr-1	45.2	52.2	86.7	32.0

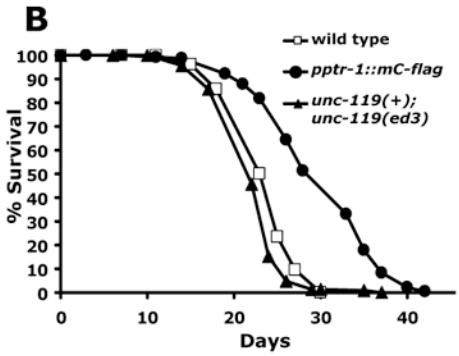

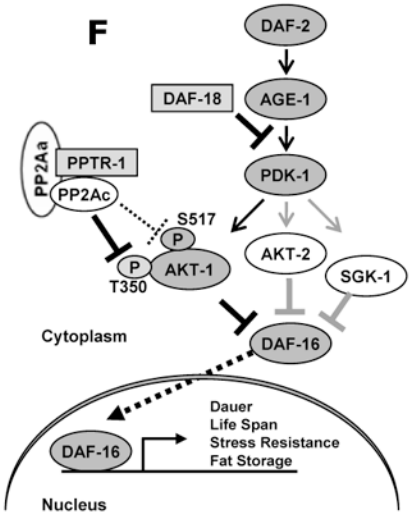

Figure 5.

PPTR-1 regulates DAF-16 localization and activity. Data shown are from one representative experiment.

A) Over-expression of PPTR-1 promotes DAF-16 nuclear translocation. On vector RNAi, DAF-16 is more enriched in the nucleus in a *pptr-1*::*mC-flag;daf-16*::*gfp* strain, compared to a *daf-16*::*gfp* strain. This effect is specific to the functional transgene, as knocking down *pptr-1*::*mC-flag* with *mCherry* RNAi decreases the extent of nuclear DAF-16.

B) Overexpression of PPTR-1 significantly increases the lifespan of wild type worms. Mean lifespan of wild type worms is 23.9 ± 0.3 days (n=154), *pptr-1*::*mC-flag* is 30.1 ± 0.5 days (n=202), p<.0001, and the *unc-119(+); unc-119(ed3)* control strain is 22.6 ± 0.3 days (n=145).

C) In a *daf-2(e1370);daf-16*::*gfp* strain, DAF-16 is enriched in the nucleus on vector RNAi, whereas on *pptr-1* RNAi as well as *daf-18* RNAi, DAf-16 is mostly cytosolic.

D) *pptr-1* RNAi affects DAF-16 transcriptional activity. *sod-3* is one of the direct targets of DAF-16. *pptr*-1 RNAi reduces *Psod-3*::GFP expression in a *daf-2(e1370);Psod-3*::*gfp (muIs84)* strain, similar to *daf-18* RNAi.

E) Transcript abundance of known DAF-16 target genes decrease when *daf-2(e1370)* worms are grown on *pptr-1* RNAi, similar to *daf-18* RNAi, as detected by real-time PCR.

F) Proposed model illustrating the role of PPTR-1 in the insulin/IGF-1 signaling pathway. Signals from DAF-2 are processed by a PI3-kinase pathway that leads to the phosphorylation and activation of downstream serine/threonine kinases such as PDK-1, AKT-1, AKT-2 and SGK-1. PPTR-1, the PP2A holoenzyme regulatory subunit, regulates the dephosphorylation and activation status of AKT-1 at T350. This in turn affects the nuclear translocation of DAF-16

and the expression of genes involved in lifespan, dauer formation, stress resistance and fat storage.

Table 1

Epistasis analysis of dauer formation using different IIS pathway mutants grown on RNAi clones

Strains	% Dauer ± Std. Dev. (n)		
	vector RNAi	***daf-18* RNAi**	***pptr-1* RNAi**
daf-2(e1368)[a]	69.2 ± 9.4 (202)	0 (295)	3.8 ± 4.4 (257)
daf-2(e1370)[b] *daf-2(e1370);daf-3(mgDf90)*	17.2 ± 5.9 (517) 94.5 ± 0.8 (589)	0.2 ± 0.3 (397) 40.4 ± 14.0 (308)	9.6 ± 7.3 (460) 42.7 ± 14.6 (329)
pdk-1(sa680)[a]	95.6 ± 1.0 (490)	80.8[c] (52)	9.5 ± 0.3 (180)
daf-2(e1370) *daf-2(e1370);akt-1(ok525)*[d] *daf-2(e1370);akt-2(ok393)*	73.0 ± 0.2 (525) 94.8 ± 3.1 (237) 36.8 ± 3.8 (336)	3.5 ± 1.7 (279) 1.0 ± 0.3 (386) 5.0 ± 1.1 (610)	4.1 ± 3.8 (344) 96.0 ± 1.7 (186) 10.8 ± 4.3 (583)
daf-2(e1370) *daf-2(e1370);sgk-1(ok538)*	79.1 ± 5.4 (601) 65.4 ± 4.9 (338)[e]	0.7 ± 1.0 (405) 0.3 ± 0.4 (303)	27.2 ± 14.8 (536) 0 (364)

All strains were maintained at 15°C and assays were performed at 20°C, unless indicated otherwise. Also, dauer formation of all strains was scored after 3.5-4 days, unless indicated otherwise. Data shown is representative of one experiment.

[a]The experiment was performed at 25 °C

[b]Dauers were scored after 5 days.

[c]In most experiments, the *pdk-1(sa680)* worms failed to hatch on *daf-18* RNAi. This number represents 20% of the eggs picked for this assay.

[d]Dauers were scored after 7-8 days. For *daf-2(e1370);akt-1(ok525)* worms on vector or *pptr-1* RNAi, all the non-dauers were either partial dauers or dauer-like. They did not develop into adults even after 2 weeks.

[e]Dauers were scored after 7-8 days. The *daf-2(e1370);sgk-1(ok538)* strain shows a gro phenotype and worms remain at the L1/L2 stage for 6-7 days at 20°C.